Nesprin-2 interacts with meckelin and mediates ciliogenesis via remodelling of the actin cytoskeleton

Helen R. Dawe[1,*], Matthew Adams[2,*], Gabrielle Wheway[2], Katarzyna Szymanska[2], Clare V. Logan[2], Angelika A. Noegel[3], Keith Gull[1] and Colin A. Johnson[2,‡]

[1]Sir William Dunn School of Pathology, University of Oxford, South Parks Road, Oxford OX1 3RE, UK
[2]Department of Ophthalmology and Neurosciences, Leeds Institute of Molecular Medicine, University of Leeds, Leeds LS9 7TF, UK
[3]Center for Biochemistry, Center for Molecular Medicine Cologne (CMMC), Cologne Excellence Cluster on Cellular Stress Responses in Aging-Associated Diseases (CECAD), Medical Faculty, University of Cologne, 50931 Cologne, Germany

*These authors contributed equally to this work
‡Author for correspondence (e-mail: c.johnson@leeds.ac.uk)

Accepted 5 May 2009
Journal of Cell Science 122, 2716-2726 Published by The Company of Biologists 2009
doi:10.1242/jcs.043794

Summary

Meckel-Gruber syndrome (MKS) is a severe autosomal recessively inherited disorder caused by mutations in genes that encode components of the primary cilium and basal body. Here we show that two MKS proteins, MKS1 and meckelin, that are required for centrosome migration and ciliogenesis interact with actin-binding isoforms of nesprin-2 (nuclear envelope spectrin repeat protein 2, also known as Syne-2 and NUANCE). Nesprins are important scaffold proteins for maintenance of the actin cytoskeleton, nuclear positioning and nuclear-envelope architecture. However, in ciliated-cell models, meckelin and nesprin-2 isoforms colocalized at filopodia prior to the establishment of cell polarity and ciliogenesis. Loss of nesprin-2 and nesprin-1 shows that both mediate centrosome migration and are then essential for ciliogenesis, but do not otherwise affect apical-basal polarity. Loss of meckelin (by siRNA and in a patient cell-line) caused a dramatic remodelling of the actin cytoskeleton, aberrant localization of nesprin-2 isoforms to actin stress-fibres and activation of RhoA signalling. These findings further highlight the important roles of the nesprins during cellular and developmental processes, particularly in general organelle positioning, and suggest that a mechanistic link between centrosome positioning, cell polarity and the actin cytoskeleton is required for centrosomal migration and is essential for early ciliogenesis.

Supplementary material available online at
http://jcs.biologists.org/cgi/content/full/122/15/2716/DC1

Key words: Centrosome, Primary cilium, Ciliogenesis, Nuclear positioning, Actin cytoskeleton, ROCK-RhoA signalling

Introduction

Meckel-Gruber syndrome (MKS) is a severe, recessively inherited developmental disorder that is characterized by bilateral renal cystic dysplasia and developmental defects of the central nervous system. MKS, and a broad phenotypic spectrum of other related syndromes, is caused by mutations in a number of genes that encode components of the primary cilium and basal body (Baala et al., 2007; Kyttala et al., 2006; Smith et al., 2006), with the aetiology presumed to arise from the defective structure or function of these organelles. MKS is therefore a member of the 'ciliopathy' class of inherited human disorders (Adams et al., 2008). Meckelin is a 995-amino-acid transmembrane protein encoded by *MKS3*, a gene commonly mutated in patients with both MKS and the related ciliopathy Joubert syndrome (JS) (Smith et al., 2006; Baala et al., 2007). Meckelin consists of an extracellular N-terminal domain, three transmembrane regions and an intracellular C-terminal domain (Smith et al., 2006) (Fig. 1A). Meckelin is predominately localized to the ciliary membrane of the primary cilium, which surrounds the axoneme of this organelle, but also has a more dispersed distribution in the apical region and at the cell surface of polarized cells (Dawe et al., 2007b). A second cause of MKS is truncating mutations in the *MKS1* gene (Kyttala et al., 2006), which encodes a basal-body protein (Kyttala et al., 2006). Our previous work has shown that MKS1 interacts with meckelin (Dawe et al., 2007b) and that both meckelin and MKS1 are required for centrosome migration to the apical cell surface during ciliogenesis (Dawe et al., 2007b). The migration of the centrosome to the apical cell surface during early cell polarization is a crucial step for ciliogenesis and the formation of primary cilia (Dawe et al., 2007a; Adams et al., 2008). Once the centrosome has migrated to and docked with the apical cell surface, it matures to form the basal body. The basal body then serves as a template for the ciliary axoneme, and cilia formation occurs via a process known as intraflagellar transport (IFT).

Nesprin-2 (nuclear envelope spectrin repeat protein 2), also known as Syne-2 (synaptic nuclear envelope protein 2) and NUANCE (nucleus and actin connecting element protein) for certain isoforms, belongs to a novel family of actin-binding proteins that localize to the outer nuclear membrane. It is a large multifunctional protein that has been implicated in mediating nuclear positioning during cellular and developmental processes (Starr and Fischer, 2005). Nesprin-2 is expressed from the *SYNE2* gene on human chromosome 14q23.2 as multiple isoforms ranging in size up to 796 kDa (Zhen et al., 2002). The N-terminus contains two actin-binding domains (ABDs), also known as calponin homology (CH) domains, whereas at least 56 spectrin repeats (Simpson and Roberts, 2008) are spread throughout the largest protein isoform, known as NUANCE or GIANT (Zhang et al., 2005) (Fig. 1B). The C-terminus of this isoform contains a single 60-amino-acid membrane-spanning region, designated the Klarsicht/ANC-1/Syne-homologue (KASH) domain, which mediates interactions with the nuclear envelope (Zhang et al., 2001; Zhen et al., 2002). The function of nesprin-2 remains unclear, but its extensive isoform diversity and multiple

Journal of Cell Science

Journal of Cell Science

subcellular locations suggest a variety of roles. In particular, a whole repertoire of ABD-containing nesprin-2 isoforms that appear to lack the transmembrane KASH domain (Zhang et al., 2005) are apparent on immunoblotting (Fig. 1C). The actin-binding CH domain and spectrin repeats are also found in several proteins that are involved in cytoskeletal and signal-transduction proteins, including actin-binding proteins such as spectrin, α-actinin and dystrophin. Nesprin-2 has been proposed to have a scaffolding function at the nuclear membrane (Libotte et al., 2005). In addition, proteins that contain the transmembrane KASH domain (including nesprin-2, its close paralogue nesprin-1 and the *Caenorhabditis elegans* protein ZYG-12) are associated with the nuclear envelope and have important roles in nuclear positioning during various cellular and developmental processes (reviewed by Starr and Fischer, 2005). In vertebrate skeletal muscle cells, the Syne-1 isoform of nesprin-1 localizes to the nuclear envelope of synaptic nuclei and seems to stably anchor them to the postsynaptic membrane at the neuromuscular junction (Grady et al., 2005).

Nesprin-2 also contains a predicted structural maintenance of chromosomes (SMC) conserved ATPase domain between amino acids 1464-1771 (Fig. 1B). The SMC domain is a well-characterized domain of proteins contained in condensin and cohesin complexes in eukaryotes, with a crucial role in both mitotic- and meiotic-chromosome segregation (Hirano, 2006), but its role in nesprin-2 is unknown. Nesprin-2 and nesprin-1 are not represented in most of the existing ciliary and basal-body proteomics data (Gherman et al., 2006), but the Syne-2 and Syne-1 isoforms have been identified as highly expressed components of the mouse photoreceptor sensory cilium proteome (Liu et al., 2007). A third member of the nesprin family, nesprin-3, lacks an ABD and instead binds to the plakin-family member plectin, which can associate with the intermediate-filament system (Wilhelmsen et al., 2005). Recently, a fourth member, nesprin-4, has been shown to interact with kinesin-1 and is proposed to contribute to microtubule-dependent nuclear and centrosome positioning (Roux et al., 2009).

Here, we demonstrate a direct in vitro interaction between meckelin and the SMC domain of actin-binding isoforms of nesprin-2. Biochemical data confirm the interaction between meckelin and nesprin-2, and also implicate MKS1 as a further interactant. Actin-binding isoforms of nesprin-2 colocalize transiently with meckelin as cells reach confluency and begin to polarize during ciliogenesis. We show, using siRNA-mediated knockdown experiments, that both nesprin-2 and nesprin-1 can contribute to centrosome migration during early cell polarization, and hence to the formation of primary cilia during the subsequent steps of ciliogenesis. Knockdown of either nesprin-2 or nesprin-1 also causes nuclear-morphology defects. Furthermore, siRNA-mediated knockdown of meckelin and *MKS3* mutations in patient fibroblasts both cause a dramatic increase in actin stress fibres and redistribution of nesprin-2 actin-binding isoforms to these fibres, as well as defects in nuclear morphology. Finally, we show that the loss of functional meckelin activates RhoA signalling, which implicates this signalling pathway in the control of the actin cytoskeleton during ciliogenesis, and suggests that meckelin and nesprin-2 are key mediators of this crucial step during cell polarization.

Results

Isoform diversity and subcellular localization of meckelin and nesprin-2 during cell polarization and ciliogenesis

First we characterized antibodies for immunodetection of nesprin-2 and meckelin by western blotting and immunofluorescence microscopy. Whole-cell extracts (WCE) were prepared from IMCD3 cells at 48 hours prior to confluence (–48 hours), confluence (0 hours) and 72 hours post-confluence (+72 hours). We used a rabbit polyclonal anti-meckelin antiserum (R29) raised against amino acids 972-985 (Fig. 1A) (Dawe et al., 2007b). The full-length isoform of meckelin (120 kDa) was present at all time points, but smaller species (80, 60 and 55 kDa) were also present at subconfluence and confluence. This might be due to post-translational protein processing to form meckelin coiled-coil-containing isoforms. A mouse monoclonal anti-nesprin-2 hybridoma-cell supernatant (K20-478; raised against the ABD of nesprin-2, amino acids 1-459, refer to Fig. 1B) (Zhen et al., 2002) detected nesprin-2 ABD-containing isoforms, including a 250-kDa isoform that was only apparent at post-confluence (+72 hours), with a second major 55-kDa isoform present both before and after confluence. A second mouse monoclonal anti-nesprin-2 antibody (K49-260; raised against spectrin repeats in the C-terminal region of nesprin-2, amino acids 6546-6796, refer to Fig. 1A) (Libotte et al., 2005) identified nesprin-2 spectrin-repeat-containing isoforms. These included a smaller 55-kDa species, but it is undetermined whether this is the same as that containing the ABD domain. Other larger spectrin-repeat-containing isoforms were present at all time points, both before and after confluence.

To compare isoform repertoire with the extent of cell polarization and ciliogenesis in IMCD3 cells, we visualized centrosomes/basal bodies and cilia over the same time course, from 48 hours prior to confluence to 72 hours post-confluence. We measured the extent of mother and daughter centriole pairing and polarization to the apical surface by immunostaining with an anti-acetylated-α-tubulin antibody to mark the ciliary axoneme, and anti-γ-tubulin antibody to mark the centrosome/basal body (supplementary material Fig. S1A). At 24 hours prior to confluence, the majority of cells were subconfluent and dividing, with mother and daughter centrioles unpaired (>5-μm apart) in 71% of cells. At +72 hours, cells were post-confluent and ciliated, with 94% of cells containing paired centrioles at the apical cell surface (supplementary material Fig. S1A). Furthermore, at +72 hours in post-confluent IMCD3 cells, we confirmed our previous observations (Dawe et al., 2007b) that meckelin is localized at the ciliary membrane and basal body, but also has a more dispersed distribution in apical regions of the cell (Fig. 1D). Immunostaining post-confluent cells at +72 hours with the anti-nesprin-2 antibody against spectrin repeats (K49-260) showed tight perinuclear localization (Fig. 1E), as previously reported (Libotte et al., 2005). We did not observe any colocalization of nesprin-2 with either meckelin, MKS1, the ciliary axoneme or the basal body in post-confluent cells (data not shown)

The C-terminal coiled-coil motif of meckelin interacts with the SMC domain of nesprin-2

To identify binding partners for meckelin, the C-terminal domain of meckelin (amino acids 751-915, including a coiled-coil motif; hereafter referred to as 'meckelin Ct') was used as a bait fragment in a GAL4 fusion construct for a yeast two-hybrid screen against preys in a human foetal brain cDNA library. Six prey clones identified nesprin-2 as a potential interacting partner, between amino acids 1370 and 1580. This region is contained within the predicted SMC domain between amino acids 1464 and 1771 of nesprin-2 (Fig. 1B). A directed 'one-to-one' yeast two-hybrid interaction assay, between the bait GAL4–meckelin-Ct fusion protein and nesprin-2 SMC-domain prey clones, confirmed that increased colony growth and size was seen for the meckelin Ct + nesprin-2 SMC-domain interaction (and for positive controls) on restrictive growth

conditions compared with negative controls (supplementary material Fig. S2).

We then transfected sub-confluent HEK 293 and IMCD3 cells with a vector encoding a HA-tagged full-length meckelin fusion protein. Transfection efficiency was approximately 60% after 48-72 hours, when cells were lysed for WCE or immunostained. HA-meckelin localized to cilia in transfected, post-confluent (+72 hr), ciliated IMCD3 cells (supplementary material Fig. S1B) and high

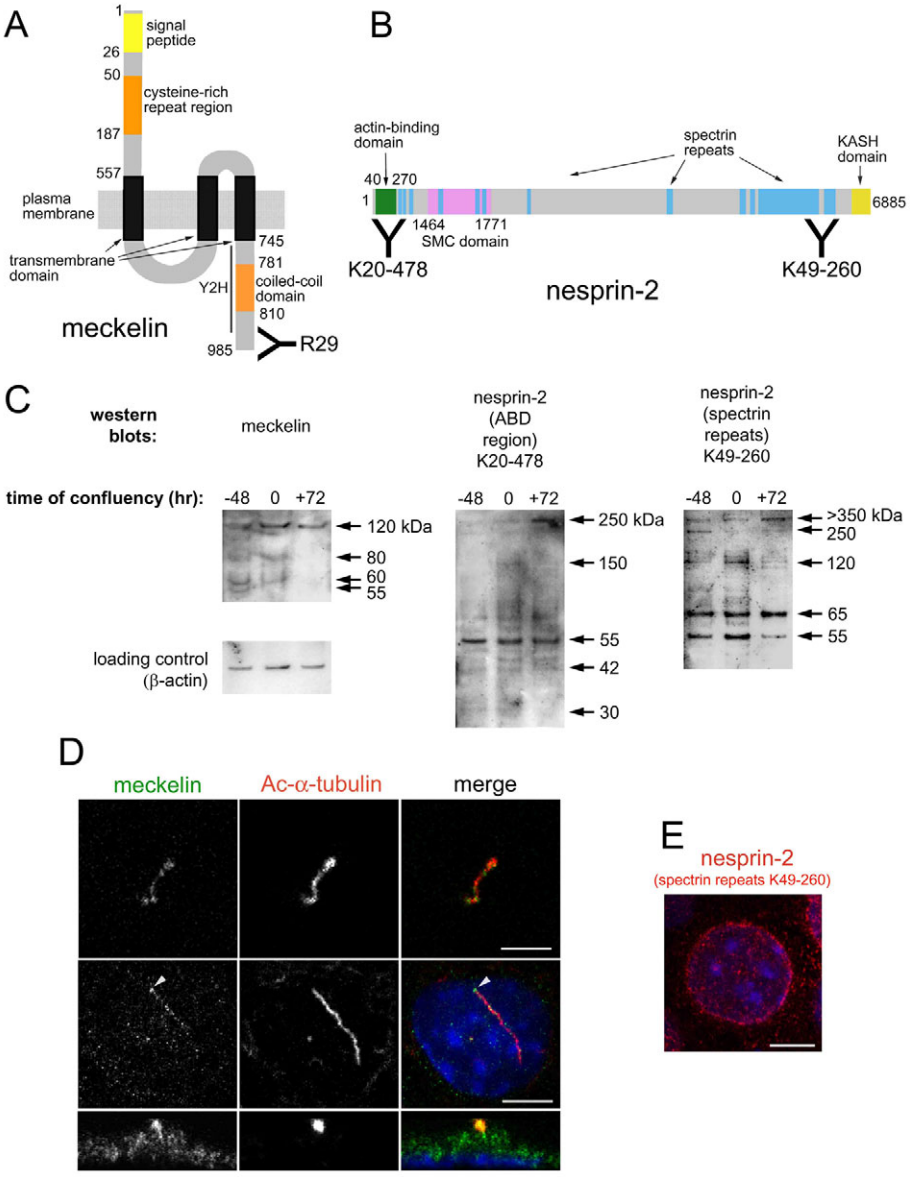

Fig. 1. Domain structures, isoform diversity and subcellular localization of meckelin and nesprin-2. (A) Domain structure of meckelin showing signal peptide, cysteine-rich-repeat region, three transmembrane domains and a coiled-coil domain. The location of the epitope for anti-meckelin antibody R29 is indicated, as is the yeast two-hybrid (Y2H) bait fragment. (B) Domain structure of the GIANT (NUANCE) isoform of nesprin-2 showing the ABD, SMC domain, spectrin-repeat regions and a transmembrane KASH domain. The locations for the epitopes of the anti-nesprin-2 antibodies K20-478 (ABD) and K49-260 (spectrin repeats) are indicated. Numbers represent amino acid residues. (C) Immunoblotting of IMCD3 WCE at 48 hours prior to confluence (–48), confluence (0) and 72 hours post-confluence (+72) with anti-meckelin antibody (R29) demonstrated that throughout ciliogenesis (–48 to +72 hours) full-length meckelin (120 kDa) was present. Smaller species of meckelin (80, 60 and 55 kDa) were also present at subconfluence and confluence. Immunoblotting with anti-nesprin-2 antibody K20-478 showed high levels of a 250-kDa ABD-containing isoform at post-confluence only, with a second major ABD-containing isoform of 55 kDa present before and after confluence. A minor 150-kDa isoform was also seen at confluence and post-confluence. Immunoblotting with anti-nesprin-2 antibody K49-260 demonstrated that a large (>350 kDa) spectrin-repeat-containing isoform persisted throughout ciliogenesis. A 250-kDa spectrin-repeat-containing isoform was present at moderate levels at subconfluence only, but other smaller species were present at all time points. An immunoblot for a loading control (β-actin) was used for each time point. (D) Co-immunostaining and confocal microscopy of ciliated IMCD3 cells at post-confluence (+72 hours) with an anti-meckelin antibody (R29; first column) and an anti-acetylated-α-tubulin antibody (second column). A merged image shows meckelin in green, acetylated-α-tubulin in red and a DAPI-labelled nucleus in blue. The upper panels show a 0.1-μm section above the apical surface of the cell showing a punctate localization of meckelin at the ciliary membrane. The middle panels are a whole-cell projection showing meckelin at the basal body (arrowhead). The bottom panels show a confocal *xz* projection through the cell monolayer, from the apical to basal surfaces. (E) Immunostaining and confocal microscopy of post-confluent (+72 hours) ciliated IMCD3 cells with anti-nesprin-2 antibody K49-260 demonstrated that spectrin-repeat-containing isoforms of nesprin-2 (red) have a perinuclear localization. The nucleus was visualized with DAPI. Scale bars: 5 μm.

Journal of Cell Science

levels of expression were confirmed by immunoblotting transfected HEK-293 WCE with an anti-HA antibody (Fig. 2A, left panel). We demonstrated a meckelin–nesprin-2 association using immunoprecipitation (IP) from transfected WCE with affinity-purified anti-nesprin-2 antibody K20-478 (Fig. 2A, right panel). An insert encoding the meckelin Ct was bacterially expressed as a GST fusion protein (supplementary material Fig. S3A). GST-pulldown experiments were performed using GST–meckelin-Ct and GST alone on WCEs, followed by immunoblotting with the anti-nesprin-2-ABD antibody (K20-478). This demonstrated a strong, direct interaction between meckelin Ct and a major 55-kDa isoform of nesprin-2 (Fig. 2B).

To confirm an interaction between endogenous meckelin and nesprin-2, we performed reciprocal IPs on WCEs from confluent cells. IP with affinity-purified anti-meckelin, followed by immunoblotting with anti-nesprin-2 (K20-478), indicated an association with two ABD-containing isoforms (150 and 250 kDa) of nesprin-2 (Fig. 2C). Other smaller isoforms were occluded by IgG heavy chain. IP with affinity-purified anti-nesprin-2 antibody against the ABD (K20-478) followed by immunoblotting with the anti-meckelin antiserum (R29) confirmed an interaction between meckelin and ABD-containing isoforms of nesprin-2 (Fig. 2D). However, IPs with the anti-nesprin-2 antibody raised against spectrin repeats (K49-260) did not detect specific interactions between meckelin and spectrin-repeat-containing isoforms of nesprin-2 (supplementary material Fig. S3B). Thus, the direct interaction of meckelin with nesprin-2 is mediated by the ABD of nesprin-2, probably by shorter isoforms that do not have the transmembrane KASH domain.

Because we have previously shown an interaction of the basal-body protein MKS1 (Kyttala et al., 2006) with meckelin (Dawe et al., 2007b), we examined a possible MKS1–nesprin-2 interaction by IP with a rabbit polyclonal anti-MKS1 antibody (Dawe et al., 2007b), followed by immunoblotting with the anti-nesprin-2 antibody against the ABD (K20-478). We found an association with nesprin-2 isoforms of the same molecular weight as those associated with meckelin (Fig. 2C). Reciprocal IP confirmed this interaction (Fig. 2E). These interactions were absent when tested with the anti-

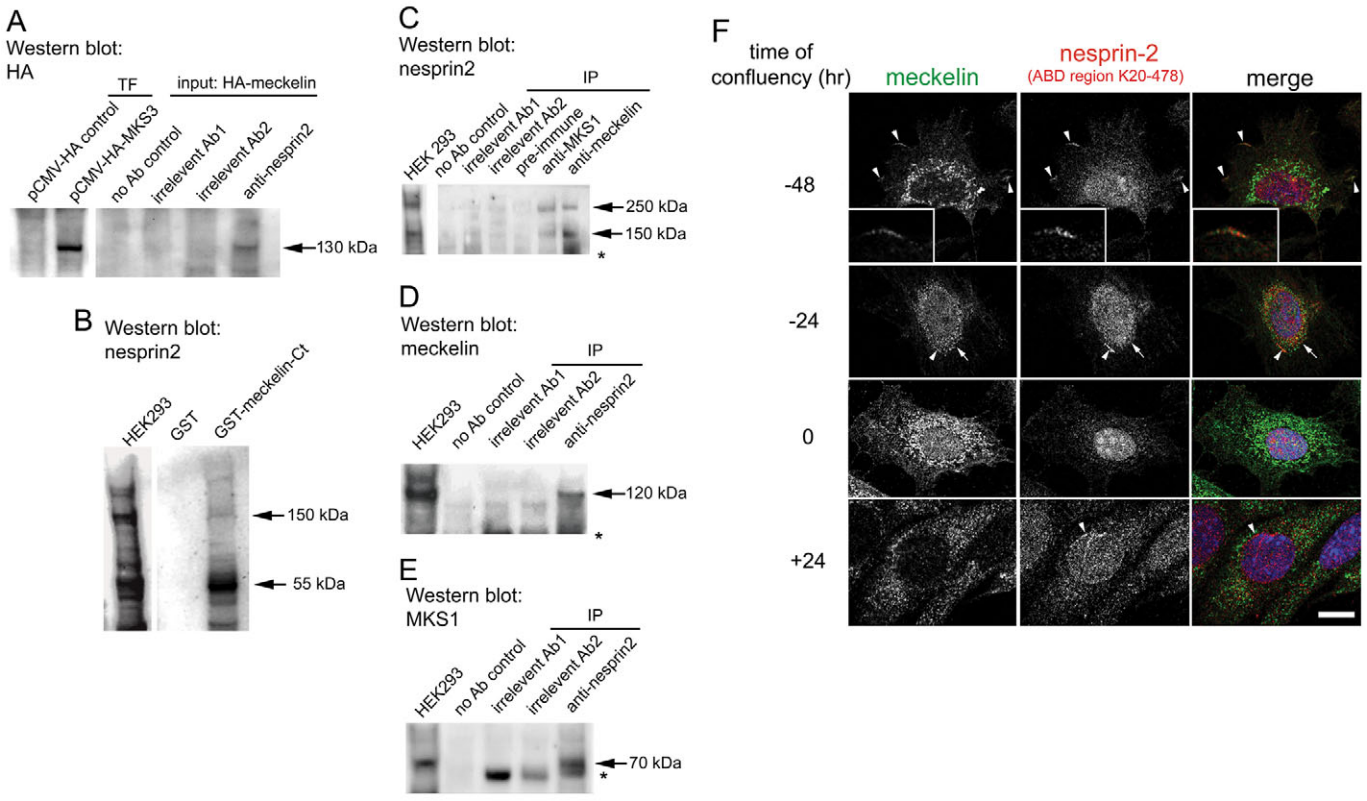

Fig. 2. Meckelin interacts with nesprin-2. (A) Immunoblotting of WCE from HA-MKS3-transfected (TF) HEK 293 cells confirmed expression of HA-tagged meckelin, at approximately 130 kDa. Immunoprecipitation (IP) of the same WCE with anti-nesprin-2 antibody against the ABD (K20-478) confirmed an interaction with HA-tagged meckelin. (B) Pulldown of ABD-containing isoforms of nesprin-2 from subconfluent HEK 293 WCE by GST-tagged meckelin C-terminus (Ct) but not by GST alone. Immunoblotting was performed using antibody K20-478. Arrows indicate 150- and 55-kDa ABD-containing isoforms of nesprin-2. HEK293 indicates 10% of total input WCE. (C) IP of ABD-containing nesprin-2 isoforms (arrows indicate 150-kDa and 250-kDa isoforms) from confluent HEK 293 WCE with anti-meckelin (R29) and anti-MKS1 but not by a no-antibody control, pre-immune serum negative control or two irrelevant antibodies (anti-parkin and anti-EFe4). HEK293 indicates 5% of total input WCE, and the asterisk (*) indicates the position of IgG heavy chain (size approximately 55 kDa). (D) IP of endogenous meckelin (arrow, size 120 kDa) from HEK 293 WCE with anti-nesprin-2 (K20-478), but not by a no-antibody control or two irrelevant antibodies. (E) IP of MKS1 (arrow, size 70 kDa) from HEK 293 WCE with anti-nesprin-2 (K20-478), but not by either a no-antibody control or the two irrelevant antibodies. (F) Subcellular localization of meckelin and nesprin-2. Co-immunostaining and confocal microscopy of IMCD3 cells at subconfluence (–48 and –24), confluence (0) and post-confluence (+24) with affinity-purified anti-meckelin antibody (green channel) and anti-nesprin-2 antibody against the ABD (K20-478, red channel). At –48 hours, a meckelin–nesprin-2 colocalization was seen at the cell periphery at probable filopodia or microspikes (arrowheads; inset shows 3× enlargement) that is absent at later time points. At –24 hours, a meckelin tubulovesicular pattern was seen that partially colocalized with nesprin-2 tubulovesicular elements (arrows). This meckelin pattern persisted, but the nesprin-2 tubulovesicular pattern was absent at confluence and post-confluence. Nesprin-2 persisted at the nucleus throughout, but perinuclear localization (arrowhead) occurred only in post-confluent ciliated cells (+24). Scale bar: 5 μm.

Journal of Cell Science

nesprin-2 antibody against spectrin repeats (K49-260; supplementary material Fig. S3B). Therefore, meckelin might exist as part of a complex with MKS1 and short, actin-binding isoforms of nesprin-2.

Meckelin and nesprin-2 colocalize prior to the establishment of cell polarity and ciliogenesis, but not in post-confluent ciliated monolayers

Although we did not observe any colocalization of nesprin-2 with meckelin in post-confluent cells (data not shown), the strong in vitro interaction data suggested that colocalization could occur in subconfluent cells during the early establishment of cell polarity and ciliogenesis. We immunostained for meckelin and for ABD-containing isoforms of nesprin-2 over the time course we had determined previously (Fig. 1C; supplementary material Fig. S1). In subconfluent cells (–48 hours prior to confluence), meckelin and nesprin-2-ABD isoforms colocalized at discrete areas along the cell periphery (Fig. 2F and insert) that contained F-actin (data not shown), suggesting that they are filopodia or microspikes. In addition, nesprin-2-ABD isoforms localized to the nucleus, and both meckelin and nesprin-2 demonstrated a tubulovesicular distribution, elements of which partially colocalized. At +24 hours post-confluence, only the meckelin tubulovesicular pattern remained, but the nesprin-2 nuclear localization persisted. At later time points (over +24 hours), nesprin-2 had the perinuclear distribution typical of post-confluent cells (Fig. 1E). MKS1 did not colocalize with nesprin-2 at any stage of the time course (data not shown) and remained at the centrosome/basal body. The results suggest that the interaction between meckelin and nesprin-2-ABD isoforms is tightly regulated, and that this association only occurs during the early establishment of cell polarity up to and including the time when cells are confluent, but not at any later stages of post-confluent cell polarization.

Loss of nesprin-2 and nesprin-1 prevent centrosome migration to the apical cell surface during early ciliogenesis

We then tested whether nesprins were required for ciliogenesis. We knocked down expression of either nesprin-1 or nesprin-2 by siRNA (Fig. 3). We used a pool of four siRNA duplexes targeted against either nesprin-1 or nesprin-2. Each pool was transiently transfected into IMCD3 cells and the presence of cilia assessed at +72 hours after cells were confluent by immunostaining with the anti-acetylated-α-tubulin antibody to mark the ciliary axoneme. We used immunoblotting with a commercial anti-nesprin-1 antibody and anti-nesprin-2 (K20-478) to determine that RNAi had been successful (Fig. 3B, arrows indicate isoforms with a reduction of approximately 50% in band intensity, consistent with the transfection efficiency of these cells). In contrast to negative-control siRNA-transfected cells, cilia formation was markedly reduced in nesprin-1- or nesprin-2-silenced cells (Fig. 3A, arrows denote the primary cilium in control cells), demonstrating that nesprin-1 and nesprin-2 could be required, either directly or indirectly, for ciliogenesis.

To test whether apical-basal polarity was perturbed by loss of nesprin-1 or nesprin-2, we performed scanning electron microscopy and assessed the presence of microvilli on the apical surface. Both nesprin-1- and nesprin-2-silenced cells formed microvilli on their cell surfaces (Fig. 3D) but, as expected, primary cilia were absent (Fig. 3D, arrows in the micrograph of control cells). Furthermore, adherens and tight junctions could also form, as shown by immunolocalization studies with antibodies against ZO-1 and E-cadherin (data not shown), suggesting that overall impairment of the establishment of apical-basal polarity is not the cause of loss of cilium formation. Because nesprins are proposed to mediate nuclear positioning in some cell types (Starr and Fischer, 2005; Roux et al., 2009), we examined whether nuclear positioning was aberrant in nesprin-1- or nesprin-2-silenced cells by analyzing thin-section transmission electron micrographs. We found no difference in the distance between the top of the nuclear envelope and the apical membrane, which remained at 1.5 μm in these cells, compared to negative-control cells. However, nuclear morphology was moderately impaired in nesprin-1-silenced cells and severely impaired in nesprin-2-silenced cells. The nuclear membrane appeared intact, but the nuclei were highly invaginated compared with negative-control cells (Fig. 3E). This nuclear defect was similar to that previously reported for nesprin silencing (Luke et al., 2008) and provides further evidence for the success of RNAi in our studies.

We have shown previously that meckelin and MKS1 are required for the initial stage of ciliogenesis (Dawe et al., 2007b), which is the migration of the centrosome to the apical cell surface. We therefore also investigated whether this early stage of ciliogenesis is also affected by loss of nesprin-1 or nesprin-2. Anti-γ-tubulin was used to mark the position of the centrosome, and the apical surface of the cell was labelled using anti-moesin (Fig. 3C). *z*-stacks were taken every 0.5 μm and cells were scored according to whether the γ-tubulin labelling was observed in an apical position (within the first 1.5 μm of the cell, above the nucleus) or deeper in the cell. γ-tubulin staining was present in the apical region of the cell in 82% of negative-control-transfected cells (Fig. 3C). By contrast, the number of cells with an apically positioned centrosome was reduced to 46% and 40% in nesprin-1- and nesprin-2-silenced cells, respectively (Fig. 3C), with a subsequent inability to form a primary cilium (Fig. 3A). Simultaneous silencing of both nesprin-1 and nesprin-2 did not have any additional effect on centrosome positioning or ciliogenesis (data not shown). These data suggest that both nesprin-1 and nesprin-2 are important determinants of centrosome/basal body positioning during cell polarization, in addition to their other known roles during organelle positioning (Starr and Fischer, 2005).

Loss of meckelin causes a ciliogenesis defect, RhoA-mediated actin cytoskeleton remodelling and redistribution of nesprin-2 to actin stress fibres

We next confirmed that siRNA-mediated knockdown of meckelin prevents ciliogenesis in IMCD3 cells at 72 hours post-confluence (Fig. 4A). Immunostaining of cells transfected with negative-control siRNA showed that meckelin had the expected tubulovesicular distribution and ABD-containing isoforms of nesprin-2 were predominately perinuclear (Fig. 4B). In IMCD3 cells following *Mks3* knockdown, meckelin levels were greatly reduced with a disperse distribution. Nesprin-2 maintained a perinuclear location, but also colocalized with actin stress fibres (Fig. 4B). We also tested nesprin-2 and meckelin localization in immortalized human embryonic fibroblasts cultured from undiseased control individuals and a patient with MKS who was compound heterozygous for the missense and truncating mutations [p.M261T]+[p.R217X] in the *MKS3* gene. MKS fibroblasts lacked cilia and had reduced levels of meckelin, as was expected from the patient genotype (Fig. 4C). Because fibroblasts have a flattened morphology, we were able to directly measure the proximity of the centrosome to the nucleus. Consistent with our previous findings in IMCD3 cells (Dawe et al., 2007b), we found that the centrosome was significantly closer to the nucleus, in either a perinuclear or apical location, for normal control cells compared with MKS fibroblasts (Fig. 4C).

In subconfluent fibroblasts, meckelin had a perinuclear and tubulovesicular pattern in control fibroblasts, and colocalized with nesprin-2 at actin-rich filapodia or microspikes (Fig. 4D). This distribution of meckelin was absent in *MKS3*-mutated cells. Most dramatically, in MKS fibroblasts nesprin-2 also colocalized with actin stress fibres at the cell periphery and within the cytoplasm (Fig. 4D) at both subconfluent (–48 hour) and post-confluent (+48 hour) time points. Because actin stress fibres in post-confluent non-migrating cells are an indication that RhoA signalling is activated (Chrzanowska-Wodnicka and Burridge, 1996; Van Aelst and Symons, 2002), we assayed levels of the RhoA-GTP activated isoform in control and MKS fibroblasts using a pulldown assay. This showed a significant (4.8-fold; $P<0.001$) increase of RhoA-GTP in MKS compared with control fibroblasts (Fig. 4E). In support of the nuclear-morphology defects seen following either nesprin-1 or nesprin-2 knockdown (Fig. 3E), similar nuclear defects were also seen in both IMCD3 cells knocked-down for *Mks3* and in the MKS fibroblasts. Defects included nuclear invaginations, blebbing and vacuolation (Fig. 4F), the incidences of which were significantly reduced in control cells.

Discussion

For ciliogenesis and the formation of primary cilia, a cell monolayer must become polarized. A crucial first step in early ciliogenesis is the migration of the centrosome to the apical cell surface during polarization, where it docks and matures to form the basal body

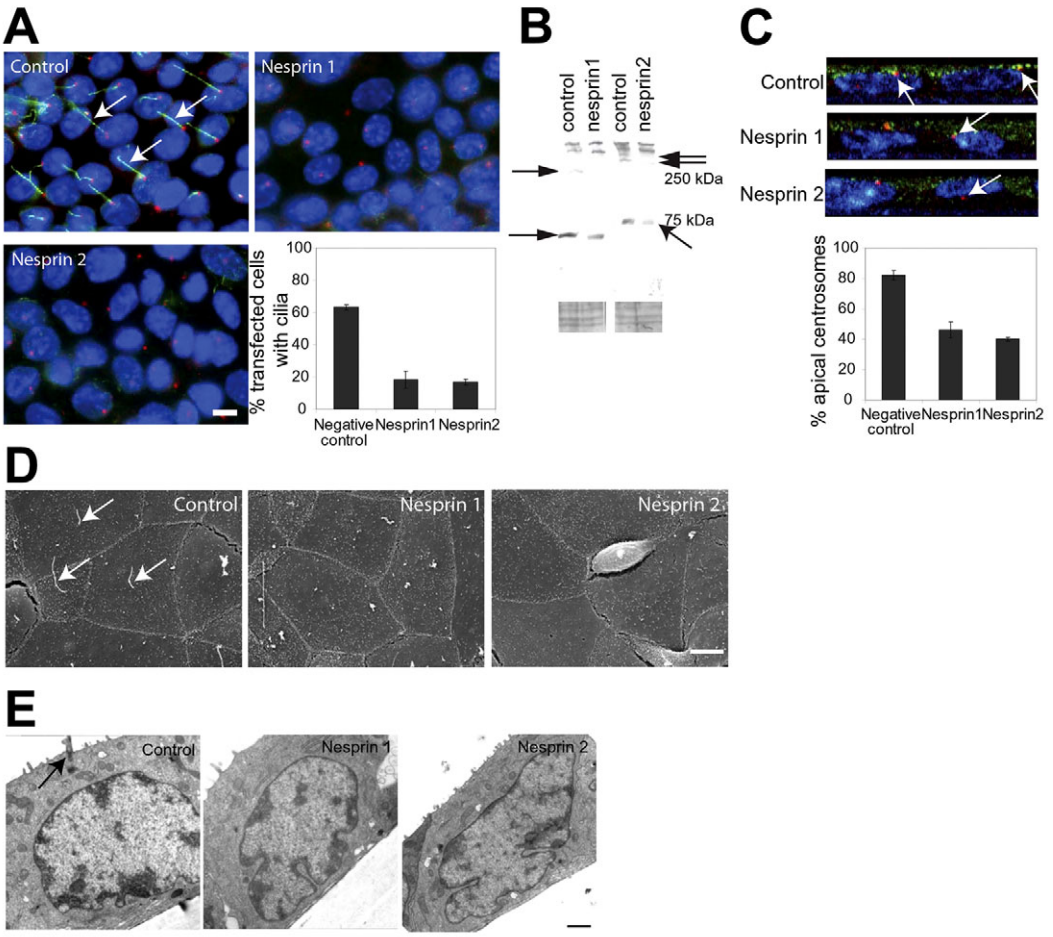

Fig. 3. Loss of nesprins prevents ciliogenesis and causes defects in nuclear morphology, but does not affect apical-basal polarity or nuclear positioning. (A) Immunofluorescence of IMCD3 monolayers transfected with negative-control siRNA, siRNA against nesprin-1 or siRNA against nesprin-2. Note the loss of primary cilia (acetylated α-tubulin staining, green) in nesprin-1 (*Syne1*)- and nesprin-2 (*Syne2*)-silenced cells compared with the negative control. DNA is labelled with DAPI (blue) and the centrosome (γ-tubulin staining) is shown in red. The graph shows quantification of the presence of a primary cilium in transfected cells, expressed as mean ± s.e.m. of three independent experiments. At least 1500 cells were counted for each condition. Scale bar: 5 µm. (B) Western blots to show the success of RNAi. Immunoblots showing certain isoforms of nesprin-1 (left panels; indicated by arrows) and isoforms of nesprin-2 that contain the ABD (right panels; arrows) are partially depleted after 96 hours of siRNA treatment, consistent with a transfection efficiency of ~60%, compared with the negative-control-transfected lane. Ponceau stain of immunoblots is shown as a loading control. (C) Confocal *xz* projections through the cell monolayer of cells (from the apical to basal surfaces); cells were transfected with negative-control siRNA (top panel), siRNA against nesprin-1 (middle panel) or siRNA against nesprin-2 (bottom panel). Cells were immunostained with anti-moesin to mark the apical cell surface (green), DAPI for DNA (blue) and anti-γ-tubulin for centrosomes (red). Note the centrosome (arrows) is deep inside the cell in nesprin-1 (*Syne1*)- and nesprin-2 (*Syne2*)-silenced cells, compared with its apical position above the nucleus in control cells. The graph shows the quantification of centrosome positioning expressed as mean ± s.e.m. of three independent experiments. At least 700 cells were counted per condition. 'Apical' is defined as the most apical 1.5-µm region of the cell. (D) Scanning electron microscopy of IMCD3 monolayers transfected with negative-control siRNA, siRNA against nesprin-1 or siRNA against nesprin-2. Microvilli form on the apical surface despite the lack of cilia. Arrows indicate primary cilia in control cells. Scale bar: 5 µm. (E) Transmission electron micrographs of control, nesprin-1 (*Syne1*)-silenced and nesprin-2 (*Syne2*)-silenced cells showing that the distance between the top of the nucleus and the apical cell surface is not affected by loss of nesprin-1 or nesprin-2. Note the primary cilium (arrow) in the control panel, and the invaginated nuclei observed on loss of nesprin-1 and especially nesprin-2. Scale bar: 1 µm.

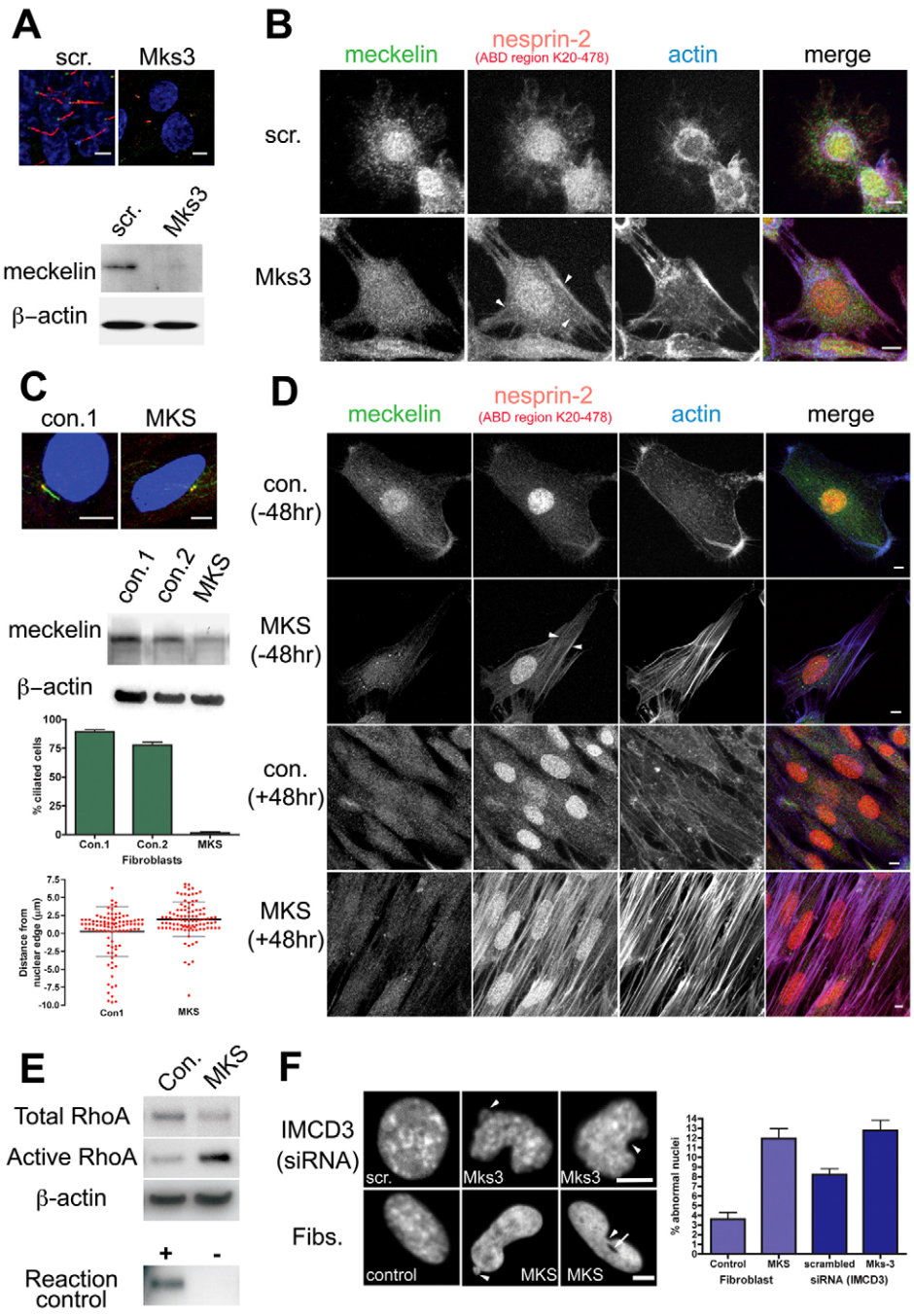

Fig. 4. See next page for legend.

(Dawe et al., 2007a; Adams et al., 2008). We have previously shown that meckelin and MKS1 are required for centrosome migration and subsequent ciliogenesis (Dawe et al., 2007b). In the present study, using a yeast two-hybrid assay, we have shown that the SMC domain of nesprin-2 interacts directly with the coiled-coil intracellular domain of meckelin (Fig. 1A,B). This interaction was confirmed in vitro by biochemical means (Fig. 2A-E) and by colocalization of actin-binding isoforms of nesprin-2 with meckelin in subconfluent cells, prior to cell polarization and ciliogenesis (Fig. 2F; supplementary material Fig. S1). Furthermore, our data suggest that nesprin-2 (and the closely related protein nesprin-1) is an important determinant of centrosome/basal body positioning during cell polarization, because loss of either meckelin or nesprin-2 prevents the correct migration of the centrosome prior to ciliogenesis, resulting in an absence of cilia formation.

Several studies have shown that nesprin proteins participate in centrosome movements, mediated by microtubule-dependent nuclear positioning (Burakov et al., 2003). The role of a physical nuclear-cytoskeletal connection, which is likely to regulate nuclear position, is further underlined by the role of the *C. elegans* ZYG-12 protein. This protein, like the nesprins, is a cytoskeletal linker protein with a KASH domain that mediates the movement of

Journal of Cell Science

Fig. 4. Subcellular phenotype of meckelin loss. (A) siRNA knockdown of Mks3 in IMCD3 cells. The top panels show IMCD3 cells co-immunostained with anti-γ-tubulin antibody (green) and an anti-acetylated-α-tubulin antibody (red). In cells transfected with scrambled siRNA control (scr.), cilia are intact, but in cells transfected with *Mks3* siRNA (Mks3), cilia are absent. DAPI staining of nuclei is shown in blue. Bottom panels show immunoblotting of WCE from cells transfected with scrambled siRNA and *Mks3* siRNA, showing loss of meckelin in the latter compared with a loading control (β-actin). Scale bars: 5 μm. (B) Subconfluent (–48 hours) IMCD3 cells co-immunostained with anti-meckelin (green), anti-nesprin-2 (K20-478; red) and phalloidin-labelled F-actin (blue). In cells transfected with scrambled siRNA control (scr.), nesprin-2 has a perinuclear distribution and meckelin a characteristic tubulovesicular pattern. In cells transfected with *Mks3* siRNA, nesprin-2 colocalized with actin stress fibres at the cell periphery and within the cytoplasm (arrowheads). Scale bars: 5 μm. (C) Subcellular phenotypes of immortalized human embryonic fibroblasts cultured from undiseased controls (con. 1 and con. 2) and an individual with Meckel-Gruber syndrome (MKS), compound heterozygous for the missense and truncating mutations [p.M261T]+[p.R217X] in *MKS3*. The top panels show control fibroblasts (con. 1) and MKS fibroblasts co-immunostained for γ-tubulin (green) and acetylated-α-tubulin (red). In control fibroblasts, cilia are intact, but in *MKS3*-mutated fibroblasts (MKS) cilia are absent. DAPI staining of nuclei is shown in blue. Immunoblots with anti-meckelin antibody and a loading control (β-actin) on WCE from two control fibroblast cell lines and MKS fibroblasts confirm a significant reduction in overall meckelin levels in *MKS3*-mutated fibroblasts compared with controls. The graph shows a cilia count in which ten high-power fields were analyzed for the presence of cilia, and confirmed significant cilia loss from MKS fibroblasts ($P<0.001$) compared with controls. In the scatter plot, the position of individual centrosomes (red dots) in multiple cells ($n=100$) is displayed relative to the edge of the nucleus. Centrosomes in control cells lie within <0.5 μm of the nucleus, whereas those in MKS fibroblasts are on average 2 μm from the nucleus ($P<0.001$; mean values are shown by black lines and s.d. in grey). Scale bars: 5 μm. (D) Subconfluent (–48hr) fibroblasts and post-confluent fibroblasts (+48hr) co-immunostained for meckelin (green), ABD-containing nesprin-2 (K20-478; red) and phalloidin (blue). In control fibroblasts (con.), nesprin-2 has a characteristic perinuclear distribution. In MKS fibroblasts, nesprin-2 also colocalized with actin stress fibres at the cell periphery and within the cytoplasm (arrowheads). This localization of nesprin-2 persists at sub- and post-confluent time points. In subconfluent (–48hr) fibroblasts, meckelin has a perinuclear and tubulovesicular pattern in control cells, and colocalizes with nesprin-2 at actin-rich filopodia or microspikes. This distribution of meckelin is absent in *MKS3*-mutated cells. Arrowheads indicate stress fibres. Scale bars: 5 μm. (E) RhoA-activation assay of normal control and MKS fibroblast WCEs showed a 4.8-fold increase in the levels of activated RhoA-GTP in patient cells. Total RhoA and β-actin are shown as loading controls. A positive control for the assay (+; loading with non-hydrolyzable GTPγS) and a negative control (–; loading with GDP) are also shown. (F) Alterations in nuclear morphology with loss of meckelin. Nuclei were labelled with DAPI. In IMCD3 cells transfected with scrambled siRNA control (scr.) and in control fibroblasts (Fibs), nuclear shape was uniformly oval (first column). In IMCD3 cells transfected with *Mks3* siRNA and in MKS fibroblasts a proportion of nuclei were abnormal, with nuclear invaginations and nuclear blebbing (arrowheads). A proportion of abnormal MKS fibroblast nuclei also contained vacuoles (arrow). Scale bars: 5 μm. The graph quantifies the proportions of abnormal nuclei in fibroblasts and in siRNA-transfected IMCD3 cells. MKS fibroblasts have significantly more abnormal nuclei ($P<0.001$), as do IMCD3 cells transfected with *Mks3* siRNA ($P<0.01$).

centrosomes towards the nucleus followed by anchoring during cell division (Malone et al., 2003). Centrosome movement, in this context, is mediated by an interaction of ZYG-12 with cytoplasmic dynein, a minus-end-directed microtubule motor. Dynein motors have also been implicated in the reorientation of the centrosome during cell polarization (Koonce et al., 1999), and the positioning of the centrosome in the cell centre (Burakov et al., 2003). However, nesprins have also been shown to interact with plus-end-directed microtubule motors, such as kinesin-2 (Fan and Beck, 2004) and kinesin-1 (Roux et al., 2009). In the latter study, nesprin-4 was found to induce kinesin-mediated cell polarization, including the apical migration of the centrosome and the basal localization of the nucleus; this observation is consistent with our findings for nesprin-2.

The actin cytoskeleton also has an active role in the repositioning of organelles such as the centrosome, nucleus and Golgi complex. In migrating fibroblasts, nuclear repositioning away from the leading edge is dependent on retrograde actin flow and myosin (Gomes et al., 2005), and the position of the centrosome is thought to be maintained by actomyosin-driven forces upon microtubules (Burakov et al., 2003). The actin cytoskeleton is also implicated in the formation of multi-ciliated epithelial cells (Boisvieux-Ulrich et al., 1990; Klotz et al., 1986; Lemullois et al., 1988; Lemullois et al., 1987) and actin enrichment at the apical cell surface is necessary for centrosome/basal body docking (Pan et al., 2007). Furthermore, activity of the Rho-GTPase regulatory factor RhoA is an essential event for actin-cytoskeletal remodelling during early mammalian ciliogenesis (Pan et al., 2007) and the Rho-associated coiled-coil-containing protein kinase p160ROCK is also required to maintain the position of the mature centriole in interphase cells (Chevrier et al., 2002). Small GTPases such as RhoA are key regulators of actin assembly and remodelling pathways, microtubule organization, membrane trafficking and transcription-factor activation during cellular and developmental processes (Van Aelst and Symons, 2002). Our results showing increased levels of the activated GTP-bound form of RhoA in MKS fibroblasts (Fig. 4E) is entirely consistent with a role for meckelin in the ROCK-RhoA signalling pathway.

It is therefore intriguing that the loss of ABD-containing isoforms of nesprin-2 (Fig. 3B) causes a complete loss of cilia (Fig. 3A). The same isoforms are also found, colocalized with meckelin, at probable filopodia or microspikes (Fig. 2F; Fig. 4B,D) of subconfluent cells. Filopodia are cytoplasmic projections that extend from the leading edge of migrating cells and contain actin filaments cross-linked into bundles by actin-binding proteins. The role of meckelin at this location is unknown, but our data demonstrate that a reduction or loss of functional meckelin causes a dramatic remodelling of the actin cytoskeleton (Fig. 4B,D), with aberrant mislocalization of nesprin-2 to actin stress fibres. We would predict that this would also cause a defect of cell migration in subconfluent cells. To support this, the phenotype of knockout mice that lack the ABD of nesprin-2 indicates that dermal fibroblasts have cell-migration and cell-polarity defects (Luke et al., 2008). Mutant fibroblast nuclei were also irregular in shape, often showing blebs at the nuclear envelope and lobulations, consistent with our observations of similar defects in cells lacking nesprin-1 or nesprin-2 (Fig. 3E), or meckelin (Fig. 4F).

Meckelin bears similarity to the Frizzled family of transmembrane Wnt receptors (Smith et al., 2006), and evidence of a signalling role stems from zebrafish embryo morphant phenotypes following morpholino knock-down of *mks3*. Defects in gastrulation movements were observed (a shortened body axis, broad notochords and misshapen somites) that are typical of defects in non-canonical (planar cell polarity) Wnt signalling (Leitch et al., 2008). The Wnt pathway has a known role in regulating a network of planar cell polarity, or PCP, genes that has RhoA as one of the downstream components (Montcouquiol et al., 2006). PCP genes are also required for the actin enrichment at the apical cell surface that is necessary for centrosome/basal body docking. In a *Xenopus laevis* model system, the disruption of the PCP genes Inturned and Fuzzy resulted in a loss of apical actin and ciliogenesis (Park et al., 2006). Both our previous work (Dawe et al., 2007b) and the present

Journal of Cell Science

study (Fig. 1D) show that meckelin is also localized to the apical region and cell surface of the cell, where it is likely to be an important component of centrosome/basal body docking. Our present study suggests that, firstly, meckelin probably regulates this process via the ROCK-RhoA signalling pathway and, secondly, that actin-binding isoforms of nesprin-2 are also components of the docking process. However, it is unclear whether the interaction between these proteins is both necessary and sufficient for this to occur. Our data also suggest that the nesprins might be an important determinant of centrosome/basal body positioning during cell polarization, because loss of either nesprin-1 or nesprin-2 prevents the correct migration of the centrosome prior to ciliogenesis (Fig. 3C). Whether centrosome migration could be mediated by nesprins having an indirect influence on either kinesin-microtubule or actomyosin-dependent movement warrants further investigation.

We therefore speculate that meckelin might act as a non-canonical Wnt receptor that mediates PCP signalling via the ROCK-RhoA pathway to cause actin-cytoskeleton rearrangements. In apical regions of the cell, such reorganization would be an essential step before the centrosome/basal body could dock and initiate ciliogenesis (Fig. 5). Nesprins have been proposed to be important for maintaining subcellular spatial organization (Zhang et al., 2005). We suggest that short actin-binding isoforms of nesprin-2 might therefore form a linking network between the centrosome and the actin cytoskeleton. By contrast, larger nesprin isoforms, which contain the KASH domain and are therefore tethered to the outer nuclear membrane, might mediate nuclear repositioning (Fig. 5). However, our siRNA reagents against nesprin-2 and nesprin-1 are not isoform-specific (Fig. 3B), so this might be an explanation why knock down has an effect on both centrosome positioning and ciliogenesis. This attractive possibility cannot be resolved by the antibodies that we have used in the present study, because these are raised against a domain rather than a particular isoform, so only further research and specific reagents will clarify this issue. The diversity of isoforms and subcellular localizations of the nesprins highlight that they are likely to be multifunctional proteins, with many unexpected roles in cell migration, cell polarity and differentiation still to be identified. Our findings provide further insight into a novel and intriguing mechanistic link between the nesprins, the actin cytoskeleton and ciliogenesis. The elucidation of the specific pathways of ciliogenesis will be important for our understanding of the aetiology of severe ciliopathies in humans, and, in the future, might suggest therapeutic interventions for conditions such as polycystic kidney disease and nephronophthisis.

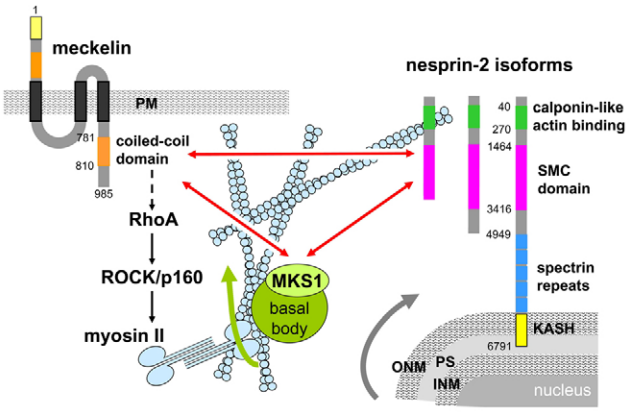

Fig. 5. Model of the interactions of MKS proteins with nesprin-2 isoforms, and their possible effects on ciliogenesis. Confirmed biochemical interactions between the coiled-coil domain of meckelin, MKS1 and nesprin-2 are shown as red arrows. Meckelin might also mediate ROCK-RhoA signalling (black arrows) to regulate the activity of myosin II and interactions with the actin cytoskeleton (pale-blue rods). Actin-cytoskeleton remodelling mediated by RhoA, and enrichment at the apical cell surface, could allow docking of the centrosome/basal body (green arrow). MKS1 (pale green) is a known component of the basal body, and interacts with both meckelin and actin-binding isoforms of nesprin-2. The domain structure of nesprin-2 is indicated (refer to Fig. 1B). Because KASH-domain-containing isoforms of nesprin-2 are also known to mediate nuclear repositioning, these isoforms could also mediate microtubule-dependent centrosome migration to the apical cell surface (grey arrow). Numbers refer to amino acid residues. PM, plasma membrane; ONM, outer nuclear membrane; PS, perinuclear space; INM, inner nuclear membrane.

Materials and Methods

Yeast two-hybrid assays

The C-terminal intracellular domain of MKS3 (meckelin; amino acids 751-915) was cloned into the lexA vector pB27 and the GAL4 vector pB6. A human foetal brain RP1 prey library was constructed. Yeast two-hybrid was performed by Hybrigenics SA as previously described (Formstecher et al., 2005; Rain et al., 2001).

Cells and antibodies

Mouse inner medullary collecting duct (IMCD3) and human embryonic kidney (HEK 293) cells were grown in Dulbecco's minimum essential medium (DMEM)/Ham's F12 supplemented with 10% foetal calf serum at 37°C/5% CO_2. Fibroblasts were immortalized with the hTERT system, and maintained in Fibroblast Growth Medium (Genlantis, San Diego, CA) supplemented with 10% foetal calf serum and 0.2 mg/ml geneticin. Normal, undiseased control fibroblasts were gestationally age-matched to fibroblasts from an MKS patient. The patient's clinical phenotype was diagnostic for MKS (posterior encephalocele, bilateral enlarged cystic kidneys, absent bladder, polydactyly of the left foot, polydactyly/syndactyly of the right foot), and the genotype was the compound heterozygous [c.653G>T]+[c.785T>C], with the coding effect of a nonsense and missense mutation on the protein of [p.R217X]+[p.M261T]. Informed consent was obtained from all participating families and the study was approved by the Leeds (East) Research Ethics Committee.

For the analysis of centrosome position, cells were grown on Transwell permeable supports (Corning). The following primary antibodies were used: rabbit anti-GST, mouse anti-HA, rabbit-anti-γ-tubulin, mouse anti-acetylated-α-tubulin (all from Sigma-Aldrich); rabbit anti-nesprin-1 and rabbit-anti-γ-tubulin (Abcam); mouse anti-E-cadherin (BD Transduction Laboratories); rat anti-ZO-1 (Zymed); anti-parkin, anti-EFe4 (both a gift from Philip Robinson, Department of Ophthalmology and Neurosciences, University of Leeds, UK); mouse anti-acetylated-α-tubulin clone C3B9, mouse-anti-nesprin-2, rabbit-anti-meckelin and rabbit anti-MKS1 have been described previously (Dawe et al., 2007b; Libotte et al., 2005; Woods et al., 1989; Zhen et al., 2002). The anti-MKS1 antibody was a gift from Nicholas Katsanis, McKusick-Nathans Institute of Genetic Medicine, Johns Hopkins University School of Medicine, Baltimore, MD. Secondary antibodies were Alexa-Fluor-488-, Alexa-Fluor-594- and Alexa-Fluor-568-conjugated goat anti-mouse IgG and goat anti-rabbit IgG (Molecular Probes). Alexa-Fluor-633–phalloidin conjugate (Molecular Probes) was used to visualize F-actin.

WCE preparation and western blotting

WCEs were prepared from subconfluent HEK 293 or IMCD3 cells. Approximately 5×10^7 cells were scraped into PBS, washed and resuspended in lysis buffer [50 mM Tris, pH 7.5, 150 mM NaCl, 0.5 mM EDTA, 0.5 mM EGTA, 0.02% (w/v) NaN_3, 1.0% (v/v) Igepal C630 (Sigma-Aldrich), 10% (v/v) glycerol, 0.1% (v/v) protease inhibitor cocktail for mammalian cell extracts in DMSO, Sigma-Aldrich]. The cell suspension was incubated on ice for 30 minutes with gentle stirring, sonicated on ice and clarified by centrifuging at 13,000 ***g*** for 5 minutes. WCEs were also prepared from transiently transfected cells for use in co-immunoprecipitation experiments (see below). WCE total protein (10 μg) was analyzed by SDS-PAGE (using 4-12% acrylamide gradient gels) and western blotting according to standard protocols. Rabbit polyclonal antisera or mouse monoclonal antibodies (mAbs) were used at final dilutions of ×200 to ×1000 for polyclonals and ×1000 to ×5000 for mAbs. Appropriate HRP-conjugated secondary antibodies (Sigma-Aldrich or Dako) were used (at ×5000 to ×10,000 dilutions) for detection by the enhanced chemiluminescence 'Femto West' western blotting detection system (Pierce) or 'Western Lightning' (Perkin Elmer).

Immunoprecipitation of immunocomplexes

WCEs were prepared from confluent untransfected HEK 293 cells, or IMCD3 cells that had been transiently transfected with 2.0 μg of plasmid DNA (empty vectors as

controls, and the pCMV-HA+MKS3 constructs as appropriate) in 90-mm tissue-culture dishes. WCE supernatants were processed for IP experiments by using 5 μg affinity-purified anti-HA (Sigma-Aldrich) or anti-nesprin-2 (Libotte et al., 2005; Zhen et al., 2002) mAbs, or 5 μg purified IgG fractions from rabbit polyclonal antisera, coupled to protein-G– and/or protein-A–Sepharose beads (GE Healthcare UK) essentially as described previously (Johnson et al., 2001).

Expression vectors, GST-pulldown and RhoA-activation assay

pGEX6P-1-GST-MKS3 (amino acids 756-986; C-terminus) was constructed by using full-length MKS3 ORF clone MGC26979 (IMAGE number 4825770) as a template in PCR, with a forward primer that contained a *Bam*HI restriction site (5′-nnnnGGATCCAGATTTATAGAAGATAAAATTCGACAG-3′), and a reverse primer with the native stop codon and an *Xho*I site (5′-nnnnCTCGAGTCAAATCAAAAATCTTTGATCCACCAA-3′), followed by sub-cloning into the pGEX6P-1 vector (GE Healthcare).

The GST fusion protein GST-meckelin (756-986; C-terminus, 'Ct') was purified from PBS/Triton X-100 extracts of sonicated *Escherichia coli* BL21 bacterial cultures. SDS-PAGE showed that the fusion protein had been packaged into inclusion bodies (not shown) following induction of protein expression with 0.5 mM IPTG. Inclusion bodies were solubilized by centrifugation of the cell lysate at 30,000 ***g*** for 30 minutes at 4°C, washing with PBS/1% Triton X-100, and addition of solubilization buffer (50 mM HEPES-NaOH, pH 7.5, 6 M guanidine, 25 mM β-mercaptoethanol) for 1 hour at 4°C. Insoluble material was removed by centrifugation at 100,000 ***g*** for 10 minutes at 12°C. The solubilized protein was refolded by rapid dilution (1:10 vol) into 50 mM HEPES, pH 7.5, 0.2 M NaCl, 1 mM β-mercaptoethanol, 1 M non-detergent sulfobetaine-201 (NDSB) at 4°C for 1 hour with stirring. Guanidine and NDSB were removed by dialysis into PBS overnight. GST fusion protein was extracted and bound from dialysate using glutathione-Sepharose-coated beads (GE Healthcare) for 1 hour with gentle agitation. For GST pulldown, HEK 293 WCE (containing 100 μg total soluble protein) was incubated with either GST or GST–meckelin-Ct–bead complexes (5 μg total protein) in incubation buffer [50 mM Tris, pH 7.5, 150 mM NaCl, 0.5 mM EDTA, 0.5 mM EGTA, 0.02% (w/v) NaN_3, 10% (v/v) glycerol, 0.1% (v/v) protease inhibitors] for 3 hours at 4°C. The bead complex was centrifuged and washed extensively with incubation buffer containing 0.1% Igepal C630 detergent, followed by SDS-PAGE and western blotting.

The activated GTP-bound isoform of RhoA was specifically assayed in pulldown assays using a GST fusion protein of the Rho effector rhotekin (Cytoskeleton, Denver, CO), using conditions recommended by the manufacturer. Cell lysates from fibroblasts were processed as rapidly as possible at 4°C and snap-frozen in liquid nitrogen. Total RhoA and pulldown protein was immunodetected on western blots using a proprietary anti-RhoA mAb (Cytoskeleton)

Transfection and siRNA

For transfection with plasmids, cells at 80% confluency were transfected with pCMV-HA or pCMV-HA-MKS3 using Fugene 6 (Roche) according to the manufacturer's instructions. Cells were incubated for 72-96 hours prior to lysis or immunostaining. For RNAi knockdown, siRNA duplexes were designed against different regions of the mouse *Mks3*, nesprin-1 (*Syne1*) or nesprin-2 (*Syne2*) sequence using Dharmacon's custom SMARTpool siRNA service. Antisense sequences were as follows: *Mks3:* 5′-UAAAUCGGAAAAUCUCUUGUU-3′, 5′-AAAUACGUUCUCCAUAUGCUU-3′, 5′-UUUCUCGCCCACUUACUGCUU-3′, 5′-CAAUCUGAAACGUCUGCCCUU-3′; nesprin-1 (*Syne1*): 5′-AAUUUAAUCGGUGAUCCUCUU-3′, 5′-AAGAACUGAUAGAAUCUCUU-3′, 5′-UGACCUGGAUGCGACGUUCUU-3′, 5′-AAAUUCCCGGCAUCGUUCUU-3′; nesprin-2 (*Syne2*): 5′-UGUCGGUGCGGUUCUCUCGUU-3′, 5′-UGUCCGUCUACGAAUUCUCUU-3′, 5′-UAUCUCGUAGGUUUUCUGUUU-3′, 5′-AAAGCCGCCAGGUCUCCUCUU-3′. The medium- or low-GC non-targeting negative controls (Invitrogen) were used as negative controls. siRNA was pooled, and 100 pmol of each pool was transfected into IMCD3 cells at 60-80% confluency using Lipofectamine 2000 (Invitrogen) according to the manufacturer's instructions. Transfected cells were identified using a fluorescent oligonucleotide transfection marker (Invitrogen); transfection efficiency was approximately 60%. Assays were carried out at 96 hours after transfection.

Electron microscopy

IMCD3 cells were grown on 13-mm glass coverslips, transfected as above and cultured for a further 4 days. Cells for transmission electron microscopy were fixed by addition of 2.5% glutaraldehyde, 2% paraformaldehyde and 0.1% picric acid in 100 mM phosphate (pH 6.5) to the culture medium followed by post-fixation in 1% osmium tetraoxide in 100 mM phosphate buffer (pH 6.5) for 1 hour at 4°C. The fixed material was stained en bloc with 2% aqueous uranyl acetate for 2 hours at 4°C. Following dehydration through a graded series of acetone and propylene oxide, the material was embedded in 'Epon' resin for sectioning. Samples fixed as above were prepared for scanning electron microscopy essentially as described (Sherwin and Gull, 1989).

Immunofluorescence and confocal microscopy

For analyses of ciliogenesis and ciliated cells, IMCD3 or fibroblast cells were seeded at 20×10^3 cells/well on glass coverslips in six-well plates and fixed in ice-cold methanol (5 minutes at 4°C) or 2% paraformaldehyde (20 minutes at room temperature) at 24-hour intervals for 7 days. For analysis of siRNA-treated cells, cells were extracted in 0.75% Triton X-100 in 100 mM PIPES, pH 6.9, 2 mM EGTA, 1 mM $MgSO_4$, 0.1 mM EDTA for 30 seconds and fixed in methanol at –20°C for at least 10 minutes. Paraformaldehyde-fixed cells were permeabilized with 0.1% Triton X-100. For immunofluorescence, cells were washed with PBS and blocked in 5% milk protein/PBS. Primary antibodies, and secondary antibodies together with DAPI (2 μg/ml), were added in 5% milk protein/PBS each for 1 hour, with further PBS washes between each stage. Primary antibodies were used at the following dilutions: mouse anti-HA (1:250); mouse anti-acetylated-α-tubulin (1:800); rabbit-anti-γ-tubulin (1:500); mouse anti-nesprin-2 (1:100), rabbit-anti-meckelin (1:50-1:250); rabbit anti-MKS1 (1:50). Secondary antibodies and phalloidin conjugate were diluted 1:500, and DAPI was diluted 1:1000. Samples were examined with a Zeiss Axioplan 2 epifluorescence microscope equipped with a motorized stage and using a 100×, 1.4 NA oil-immersion lens, and images were captured with a CCD camera (Coolsnap HQ, Photometrics) controlled by Metamorph (Universal Imaging). Confocal images were obtained using either Nikon Eclipse TE2000-E or Zeiss LSM510 META confocal imaging systems, controlled by either LSM software (Zeiss) or EZ-C1 3.50 (Nikon) software. Images were processed in Metamorph and figures were assembled using Adobe Photoshop CS3.

We thank Mike Shaw (University of Oxford) for assistance with electron microscopy, and Eva Pitt (Cancer Research UK, St James's University Hospital) for help with tissue culture. This work was funded by the Medical Research Council (project grant G0700073), the Wellcome Trust, the E. P. Abraham Trust and the Beit Memorial Fellowships for Medical Research. H.R.D. is a Beit Memorial Research Fellow, and K.G. is a Wellcome Trust Principal Research Fellow. Deposited in PMC for release after 6 months.

References

Adams, M., Smith, U. M., Logan, C. V. and Johnson, C. A. (2008). Recent advances in the molecular pathology, cell biology and genetics of ciliopathies. *J. Med. Genet.* **45**, 257-267.

Baala, L., Romano, S., Khaddour, R., Saunier, S., Smith, U. M., Audollent, S., Ozilou, C., Faivre, L., Laurent, N., Foliguet, B. et al. (2007). The Meckel-Gruber syndrome gene, MKS3, is mutated in Joubert syndrome. *Am. J. Hum. Genet.* **80**, 186-194.

Boisvieux-Ulrich, E., Laine, M. and Sandoz, D. (1990). Cytochalasin D inhibits basal body migration and ciliary elongation in quail oviduct epithelium. *Cell Tissue Res.* **259**, 443-454.

Burakov, A., Nadezhdina, E., Slepchenko, B. and Rodionov, V. (2003). Centrosome positioning in interphase cells. *J. Cell Biol.* **162**, 963-969.

Chevrier, V., Piel, M., Collomb, N., Saoudi, Y., Frank, R., Paintrand, M., Narumiya, S., Bornens, M. and Job, D. (2002). The Rho-associated protein kinase p160ROCK is required for centrosome positioning. *J. Cell Biol.* **157**, 807-817.

Chrzanowska-Wodnicka, M. and Burridge, K. (1996). Rho-stimulated contractility drives the formation of stress fibers and focal adhesions. *J. Cell Biol.* **133**, 1403-1415.

Dawe, H. R., Farr, H. and Gull, K. (2007a). Centriole/basal body morphogenesis and migration during ciliogenesis in animal cells. *J. Cell Sci.* **120**, 7-15.

Dawe, H. R., Smith, U. M., Cullinane, A. R., Gerrelli, D., Cox, P., Badano, J. L., Blair-Reid, S., Sriram, N., Katsanis, N., Attie-Bitach, T. et al. (2007b). The Meckel-Gruber Syndrome proteins MKS1 and meckelin interact and are required for primary cilium formation. *Hum. Mol. Genet.* **16**, 173-186.

Fan, J. and Beck, K. A. (2004). A role for the spectrin superfamily member Syne-1 and kinesin II in cytokinesis. *J. Cell Sci.* **117**, 619-629.

Formstecher, E., Aresta, S., Collura, V., Hamburger, A., Meil, A., Trehin, A., Reverdy, C., Betin, V., Maire, S., Brun, C. et al. (2005). Protein interaction mapping: a Drosophila case study. *Genome Res.* **15**, 376-384.

Gherman, A., Davis, E. E. and Katsanis, N. (2006). The ciliary proteome database: an integrated community resource for the genetic and functional dissection of cilia. *Nat. Genet.* **38**, 961-962.

Gomes, E. R., Jani, S. and Gundersen, G. G. (2005). Nuclear movement regulated by Cdc42, MRCK, myosin, and actin flow establishes MTOC polarization in migrating cells. *Cell* **121**, 451-463.

Grady, R. M., Starr, D. A., Ackerman, G. L., Sanes, J. R. and Han, M. (2005). Syne proteins anchor muscle nuclei at the neuromuscular junction. *Proc. Natl. Acad. Sci. USA* **102**, 4359-4364.

Hirano, T. (2006). At the heart of the chromosome: SMC proteins in action. *Nat. Rev. Mol. Cell Biol.* **7**, 311-322.

Johnson, C. A., Padget, K., Austin, C. A. and Turner, B. M. (2001). Deacetylase activity associates with topoisomerase II and is necessary for etoposide-induced apoptosis. *J. Biol. Chem.* **276**, 4539-4542.

Klotz, C., Bordes, N., Laine, M. C., Sandoz, D. and Bornens, M. (1986). Myosin at the apical pole of ciliated epithelial cells as revealed by a monoclonal antibody. *J. Cell Biol.* **103**, 613-619.

Koonce, M. P., Köhler, J., Neujahr, R., Schwartz, J. M., Tikhonenko, I. and Gerisch, G. (1999). Dynein motor regulation stabilizes interphase microtubule arrays and determines centrosome position. *EMBO J.* **18**, 6786-6792.

Kyttala, M., Tallila, J., Salonen, R., Kopra, O., Kohlschmidt, N., Paavola-Sakki, P., Peltonen, L. and Kestila, M. (2006). MKS1, encoding a component of the flagellar

apparatus basal body proteome, is mutated in Meckel syndrome. *Nat. Genet.* **38**, 155-157.

Leitch, C. C., Zaghloul, N. A., Davis, E. E., Stoetzel, C., Diaz-Font, A., Rix, S., Alfadhel, M., Lewis, R. A., Eyaid, W., Banin, E. et al. (2008). Hypomorphic mutations in syndromic encephalocele genes are associated with Bardet-Biedl syndrome. *Nat. Genet.* **40**, 443-448.

Lemullois, M., Klotz, C. and Sandoz, D. (1987). Immunocytochemical localization of myosin during ciliogenesis of quail oviduct. *Eur. J. Cell Biol.* **43**, 429-437.

Lemullois, M., Boisvieux-Ulrich, E., Laine, M. C., Chailley, B. and Sandoz, D. (1988). Development and functions of the cytoskeleton during ciliogenesis in metazoa. *Biol. Cell* **63**, 195-208.

Libotte, T., Zaim, H., Abraham, S., Padmakumar, V. C., Schneider, M., Lu, W., Munck, M., Hutchison, C., Wehnert, M., Fahrenkrog, B. et al. (2005). Lamin A/C-dependent localization of Nesprin-2, a giant scaffolder at the nuclear envelope. *Mol. Biol. Cell* **16**, 3411-3424.

Liu, Q., Tan, G., Levenkova, N., Li, T., Pugh, E. N., Jr, Rux, J. J., Speicher, D. W. and Pierce, E. A. (2007). The proteome of the mouse photoreceptor sensory cilium complex. *Mol. Cell Proteomics* **6**, 1299-1317.

Luke, Y., Zaim, H., Karakesisoglou, I., Jaeger, V. M., Sellin, L., Lu, W., Schneider, M., Neumann, S., Beijer, A., Munck, M. et al. (2008). Nesprin-2 Giant (NUANCE) maintains nuclear envelope architecture and composition in skin. *J. Cell Sci.* **121**, 1887-1898.

Malone, C. J., Misner, L., Le Bot, N., Tsai, M. C., Campbell, J. M., Ahringer, J. and White, J. G. (2003). The C. elegans hook protein, ZYG-12, mediates the essential attachment between the centrosome and nucleus. *Cell* **115**, 825-836.

Montcouquiol, M., Crenshaw, E. B., 3rd. and Kelley, M. W. (2006). Noncanonical Wnt signaling and neural polarity. *Annu. Rev. Neurosci.* **29**, 363-386.

Pan, J., You, Y., Huang, T. and Brody, S. L. (2007). RhoA-mediated apical actin enrichment is required for ciliogenesis and promoted by Foxj1. *J. Cell Sci.* **120**, 1868-1876.

Park, T. J., Haigo, S. L. and Wallingford, J. B. (2006). Ciliogenesis defects in embryos lacking inturned or fuzzy function are associated with failure of planar cell polarity and Hedgehog signaling. *Nat. Genet.* **38**, 303-311.

Rain, J. C., Selig, L., De Reuse, H., Battaglia, V., Reverdy, C., Simon, S., Lenzen, G., Petel, F., Wojcik, J., Schachter, V. et al. (2001). The protein-protein interaction map of Helicobacter pylori. *Nature* **409**, 211-215.

Roux, K. J., Crisp, M. L., Liu, Q., Kim, D., Kozlov, S., Stewart, C. L. and Burke, B. (2009). Nesprin 4 is an outer nuclear membrane protein that can induce kinesin-mediated cell polarization. *Proc. Natl. Acad. Sci. USA* **106**, 2194-2199.

Sherwin, T. and Gull, K. (1989). The cell division cycle of Trypanosoma brucei brucei: timing of event markers and cytoskeletal modulations. *Philos. Trans. R. Soc. Lond. B Biol. Sci.* **323**, 573-588.

Simpson, J. G. and Roberts, R. G. (2008). Patterns of evolutionary conservation in the nesprin genes highlight probable functionally important protein domains and isoforms. *Biochem. Soc. Trans.* **36**, 1359-1367.

Smith, U. M., Consugar, M., Tee, L. J., McKee, B. M., Maina, E. N., Whelan, S., Morgan, N. V., Goranson, E., Gissen, P., Lilliquist, S. et al. (2006). The transmembrane protein meckelin (MKS3) is mutated in Meckel-Gruber syndrome and the wpk rat. *Nat. Genet.* **38**, 191-196.

Starr, D. A. and Fischer, J. A. (2005). KASH 'n Karry: the KASH domain family of cargo-specific cytoskeletal adaptor proteins. *BioEssays* **27**, 1136-1146.

Van Aelst, L. and Symons, M. (2002). Role of Rho family GTPases in epithelial morphogenesis. *Genes Dev.* **16**, 1032-1054.

Wilhelmsen, K., Litjens, S. H., Kuikman, I., Tshimbalanga, N., Janssen, H., van den Bout, I., Raymond, K. and Sonnenberg, A. (2005). Nesprin-3, a novel outer nuclear membrane protein, associates with the cytoskeletal linker protein plectin. *J. Cell Biol.* **171**, 799-810.

Woods, A., Sherwin, T., Sasse, R., MacRae, T. H., Baines, A. J. and Gull, K. (1989). Definition of individual components within the cytoskeleton of Trypanosoma brucei by a library of monoclonal antibodies. *J. Cell Sci.* **93**, 491-500.

Zhang, Q., Skepper, J. N., Yang, F., Davies, J. D., Hegyi, L., Roberts, R. G., Weissberg, P. L., Ellis, J. A. and Shanahan, C. M. (2001). Nesprins: a novel family of spectrin-repeat-containing proteins that localize to the nuclear membrane in multiple tissues. *J. Cell Sci.* **114**, 4485-4498.

Zhang, Q., Ragnauth, C. D., Skepper, J. N., Worth, N. F., Warren, D. T., Roberts, R. G., Weissberg, P. L., Ellis, J. A. and Shanahan, C. M. (2005). Nesprin-2 is a multi-isomeric protein that binds lamin and emerin at the nuclear envelope and forms a subcellular network in skeletal muscle. *J. Cell Sci.* **118**, 673-687.

Zhen, Y. Y., Libotte, T., Munck, M., Noegel, A. A. and Korenbaum, E. (2002). NUANCE, a giant protein connecting the nucleus and actin cytoskeleton. *J. Cell Sci.* **115**, 3207-3222.

Journal of Cell Science